

**Figure 1.** A computer-generated perspective drawing of octalactin A. No absolute configuration is implied.

cell lines. Fractionation of the crude extract by silica vacuum flash chromatography followed by silica HPLC (EtOAc/isooctane, 7/3) yielded octalactins A (1) and B (2) in variable ratios at less than 1% of the organic extract. Octalactin A (1), mp 155–157 °C, analyzed for  $C_{19}H_{32}O_6$  by high-resolution mass spectrometry and  $^{13}C$  NMR.<sup>10</sup> The  $^{13}C$  NMR spectrum of 1 showed a ketone carbonyl resonance at  $\delta$  212.4 ppm and an ester carbonyl at  $\delta$  172.4 ppm. Resonances attributed to two secondary alcohols ( $\delta$  71.3 and 74.5 ppm, both CH), to the non-carbonyl carbon of the lactone ( $\delta$  79.3, CH), and to a trisubstituted epoxide ( $\delta$  62.4 ppm, C, and 58.8 ppm, CH) were also observed, thus accounting for all the oxygens in 1. A combination of COSY  $^1H$  NMR and XHCORR and COLOC  $^{13}C$  NMR experiments<sup>10</sup> defined the planar, but not the three-dimensional, structure of 1. The relative stereostructure of 1 was established by single-crystal X-ray crystallographic methods,<sup>11</sup> and a computer-generated perspective drawing is shown in Figure 1.

Octalactin A contains an unusual eight-membered lactone moiety.<sup>6–8</sup> As can be seen in Figure 1, the lactone ring has a boat-chair conformation with a cis lactone (C7–O1–C1–C2:  $-0.8$  ( $6^\circ$ ) in the solid state. Earlier molecular mechanics calculations<sup>12,13</sup> of eight-membered lactone rings indicated four local minima within 1.31 kcal/mol of the ground state. Calculations on a trisubstituted eight-membered lactone ring model of 1, using Monte Carlo searching of conformation space with the BATCHMIN subroutine of MACROMODEL<sup>14</sup> and the MM2 force field, show six distinct minima (supplementary material) within 0.95 kcal/mol of the ground state. One of these conformations, the lower boat-chair, was that found in the X-ray study. Of the six conformations, five are cis lactones, while the sixth, with the highest calculated steric energy in vacuum, is trans. Due to the larger dipole moment of the cis conformers, they are predicted to be significantly stabilized in polar solution. Strong intermo-

lecular hydrogen bonding between the lactone carbonyl, the C3 hydroxyl, and the C13 hydroxyl in the crystal structure could be responsible for the solid-state conformation.

Octalactin B (2) was isolated as a colorless oil. Analysis of  $^{13}C$  and  $^1H$  NMR data showed 2 to be the corresponding C10–C11 olefin derivative of 1.<sup>15</sup> Octalactin A was responsible for most of the cytotoxic activity of the extract and displayed  $IC_{50}$  values of  $7.2 \times 10^{-3}$   $\mu g/mL$  (B-16-F10) and 0.5  $\mu g/mL$  (HCT-116). Octalactin B was completely inactive in the cytotoxicity assays against murine and human cancer cell lines.

**Acknowledgment.** This research was funded by the PHS, National Institutes of Health, and through the National Cancer Institute under Grants CA44848 (W.F.) and CA24487 (J.C.). We thank the Bristol-Myers Squibb Company for providing in vitro cancer cell cytotoxicity bioassays.

**Registry No.** 1, 133473-06-0; 2, 133473-07-1.

**Supplementary Material Available:** Tables of fractional coordinates, thermal parameters, interatomic distances, bond angles, and torsional angles for octalactin A (1) and a summary figure of low-energy conformations (5 pages). Ordering information is given on any current masthead page.

(15) Octalactin B (2), an oil, showed  $[\alpha]_D -12.3^\circ$  (c 5.6,  $CHCl_3$ ), analyzed for  $C_{19}H_{32}O_5$  by HRMS (obsd  $M^+ m/z$  341.2211, calcd 341.2328), and showed the following spectral features: IR (neat 3450, 1715, 1660, 1460, 1380  $cm^{-1}$ );  $^1H$  NMR (360 MHz,  $CDCl_3$ )  $\delta$  3.05 (dd, 13.3, 1.8) and 2.73 (dd, 13.3, 6.1) both C2, 4.04 (br s) C3, 1.60 (m) C4, 1.65 (m) and 1.23 (m) both C5, 1.80 (m) and 1.70 (m) both C6, 4.76 (br t, 9.7) C7, 3.55 (dq, 7.2, 7.2) C8, 6.87 (t, 6.8) C11, 2.45 (ddd, 1.51, 6.8, 3.6) C12, 3.52 (br s) C13, 1.70 (m) C14, 1.14 (d, 7.2) C15, 0.96 (d, 6.8) C16, 1.78 (s) C17, 1.05 (d, 7.2) C18, 0.97 (d, 6.8) C19;  $^{13}C$  NMR (50 MHz,  $CDCl_3$ )  $\delta$  172.6, 39.2, 71.4, 33.9, 22.7, 32.2, 79.4, 44.3, 203.3, 137.5, 141.4, 34.1, 75.8, 38.0, 22.0, 18.7, 11.7, 14.9, 17.4 for C1 to C19, respectively.

## Conformational Change of Cholesterol Side Chain in Lipid Bilayers

Wen-guey Wu\* and Lang-Ming Chi

*Institute of Life Sciences  
National Tsing Hua University, Hsinchu, Taiwan 30043  
Republic of China*

Received November 7, 1990

The cholesterol-lipid interactions at the molecular level have been attributed primarily to the hydrogen-bond formation of the  $\beta$ -hydroxyl group and the hydrophobic steric contact of the condensed steroid ring.<sup>1,2</sup> It is not clear how the cholesterol side chain interacts with lipid molecules, although sterols containing shortened or lengthened side chains are less effective in modulating bilayer fluidity.<sup>2</sup> In this communication, we provide solid-state NMR evidence to indicate that the  $\omega_4$  ( $C_{22}$ – $C_{23}$ – $C_{24}$ – $C_{25}$ ) torsion angle of the cholesterol side chain depends on the chain length of the neighboring lysophosphatidylcholine (LPC) molecules.

Equimolar mixtures of LPC (16:0) and cholesterol are known to form lamellar structures in aqueous media as a consequence of some specific 1:1 LPC-cholesterol complex formation.<sup>3–5</sup> The  $^{31}P$  NMR results shown in Figure 1A suggest a similar LPC-cholesterol complex formation for the four studied LPC/cholesterol

(10) Octalactin A (1), mp 155–157 °C ( $CHCl_3$ /EtOAc), showed  $[\alpha]_D -14^\circ$  (c 1.8,  $CHCl_3$ ), analyzed for  $C_{19}H_{32}O_6$  by HRMS (obsd  $M^+ m/z$  357.2264, calcd 357.2277), and showed the following spectral features: IR (neat) 3450, 1720  $cm^{-1}$ ;  $^1H$  NMR (360 MHz,  $CDCl_3$ , assignments by COSY methods)  $\delta$  2.97 (br d, 13.3) and 2.72 (dd, 13.3, 6.1) both C2, 4.03 (br s) C3, 4.60 (t, 9.7) C7, 2.96 (m) C8, 3.55 (t, 6.1) C11, 1.78 (m) C12, 3.50 (m) C13, 1.13 (d, 6.8) C15, 0.92 (d, 6.8) C16, 1.44 (s) C17, 1.00 (d, 6.8) C18, 0.94 (d, 6.8) C19; unlisted protons were part of an unresolved multiplet;  $^{13}C$  NMR (50 MHz,  $CDCl_3$ , assignments by XHCORR and COLOC methods)  $\delta$  172.4, 39.3, 71.3, 34.0, 22.5, 32.0, 79.3, 42.5, 212.4, 62.4, 58.8, 32.3, 74.5, 38.0, 22.0, 18.4, 12.6, 13.4, 17.6 for C1 to C19, respectively.

(11) Octalactin A (1) crystallized in the orthorhombic space group  $P2_12_12_1$ , with  $a = 9.965$  (2) Å,  $b = 21.010$  (4) Å,  $c = 9.701$  (3) Å, and one molecule of composition  $C_{19}H_{32}O_6$  in the asymmetric unit. Diffraction maxima were measured by using  $2\theta$ - $\theta$  scans and graphite-monochromated Cu K $\alpha$  radiation to a  $2\theta$  limit of  $114^\circ$ . Of the 1583 reflections collected in this way, 1503 (95%) were judged observed ( $|F_o| \geq 4\sigma(|F_o|)$ ). The structures was solved by direct methods (MULTAN) and refined by using full-matrix least-squares analysis of 25 anisotropic heavy atoms and 32 riding model, isotropic hydrogens to a standard crystallographic discrepancy ratio of 0.0525. Additional crystallographic details are available and are described under Supplementary Material Available.

(12) Allinger, N. L. *Pure Appl. Chem.* **1982**, *54*, 2515–2522.

(13) Burkert, U.; Allinger, N. L. *Molecular Mechanics*; ACS Monograph 177; American Chemical Society: Washington, DC, 1982.

(14) Mohamadi, F.; Richards, N. G. J.; Guida, W. C.; Liskamp, R.; Lip-ton, M.; Caufield, C.; Chang, G.; Hendrickson, T.; Still, W. C. *J. Comput. Chem.* **1990**, *11*, 440–467.

(1) Huang, C. *Lipids* **1977**, *12*, 348–356.

(2) Block, K. In *Biochemistry of Lipids and Membranes*; Vance and Vance, Eds.; Benjamin/Cummings Co.: Menlo Park, CA, 1985; Chapter 1.

(3) Rand, R. P.; Pangborn, W. A.; Purdon, A. D.; Tinker, D. O. *Can. J. Biochem.* **1975**, *53*, 189–195.

(4) Wu, W., Stephenson, F. A.; Mason, J. T.; Huang, C. *Lipids* **1984**, *19*, 68–71.

(5) Killian, J. A.; Borle, F.; de Kruijff, B.; Seelig, J. *Biochim. Biophys. Acta* **1986**, *854*, 133–142.

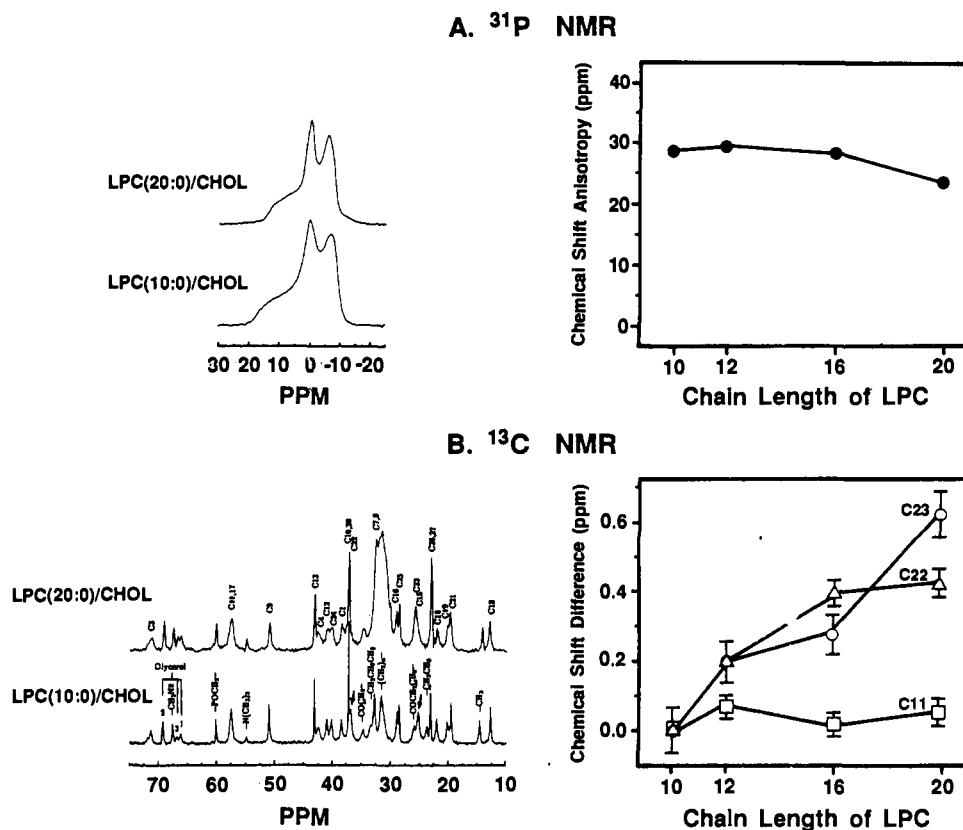


**Figure 1.** Solid-state NMR studies on the 1/1 molar ratio of LPC/cholesterol dispersions at 30 °C. (A) Representative  $^{31}\text{P}$  NMR spectra and the determined chemical shift anisotropy of the indicated LPC/cholesterol mixtures. A Hahn echo with phase recycle in the presence of proton decoupling was used. The repetition time was typically 5 s. Chemical shifts were relative to 85%  $\text{H}_3\text{PO}_4$ . The isotropic peak was due to the presence of LPC/cholesterol liposomes with smaller diameters. A similar isotropic peak has previously been observed by  $^2\text{H}$  and  $^{14}\text{N}$  NMR.<sup>4,5</sup> The area under the isotropic peak is generally less than 10% of the total area under the anisotropic spectrum. The lipids were checked by thin-layer chromatography with chloroform/methanol/water (65/25/4, by volume) as eluent. Only one single spot was detected for each lipid. The axial symmetric  $^{31}\text{P}$  NMR spectra suggest that all the studied LPC/cholesterol mixtures exhibit similar lamellar structures. (B) Representative  $^{13}\text{C}$  NMR spectra and the determined  $^{13}\text{C}$  chemical shift differences of the 1/1 molar ratio of LPC/cholesterol mixtures at 30 °C. The spectra were obtained with a Bruker MSL-200 NMR spectrometer by a single contact cross-polarization pulse sequence in conjunction with magic angle spinning. The contact time for the spectra shown in the figure was 4 ms. Each spectrum was typically 2000 scans with a 5-s delay time and a 4- $\mu\text{s}$  90° pulse. The chemical shifts were referenced to external tetramethylsilane. The error bars represent the standard deviation obtained from the average of 10 measurements at different contact times. Attention is drawn to the upfield displacement of the  $\text{C}_{22}$  and  $\text{C}_{23}$  signals in the cholesterol side chain of the LPC(10:0)/cholesterol mixture. Representative values of the  $\text{C}_{11}$  signal were also plotted against the chain length of LPC molecules to indicate the relatively constant chemical shift values of the  $^{13}\text{C}$  signals from the cholesterol condensed ring.

mixtures. All the  $^{31}\text{P}$  NMR spectra exhibited a characteristic axial symmetric anisotropic line shape with similar chemical shift anisotropy values. This indicates that the lamellar structures formed by the LPC-cholesterol complex do not depend on the phase properties of single-component LPC dispersions<sup>6</sup> and are suitable for the study of cholesterol-lipid interaction.

Molecular properties of the LPC-cholesterol complex were further studied by cross-polarization/magic angle spinning  $^{13}\text{C}$  NMR<sup>7,8</sup> as shown in Figure 1B. Most of the  $^{13}\text{C}$  NMR signals can be assigned according to recent reports.<sup>6,9</sup> The  $\text{C}_{22}$  and  $\text{C}_{23}$  signals of the cholesterol side chain were found to be superimposed with other cholesterol or LPC signals for the LPC(20:0)/cholesterol mixture, but they became resolvable for the LPC(10:0)/cholesterol mixture (see the two arrows shown in Figure 1B). Variation of the temperature from 30 °C to 50 °C did not produce spectral change for the LPC(20:0)/cholesterol mixture (data not shown) despite the fact that the LPC(20:0) dispersion showed a phase transition at 45 °C. The relative assignments of the  $\text{C}_{22}$  and  $\text{C}_{23}$  signals can be done by examining the relaxation behavior of each peak as a function of contact time and by reasonably

assuming that the cholesterol condensed ring signals remain unchanged in their resonance positions for the four studied mixtures. Measurement of the effect of contact time on the spectral intensity is in effect an indirect measurement of the rotating frame proton spin-lattice relaxation time ( $T_{1\rho}$ ).<sup>8</sup> Characteristic different  $T_{1\rho}$  values were observed for the carbon atoms of cholesterol and phospholipid molecules.<sup>6</sup> According to this assignment, the chemical shifts of the indicated cholesterol side chain  $^{13}\text{C}$  signals increased with the chain length of phospholipid in LPC/cholesterol mixtures.

Figure 2 shows the chemical shift differences (close symbols) and the  $T_{1\rho}$  values (open symbols) of the cholesterol signals for LPC(20:0)/cholesterol and LPC(10:0)/cholesterol mixtures as a function of the carbon position of the cholesterol molecule. Consistent with previous dynamic studies of the cholesterol side chain in lipid bilayers,<sup>10-12</sup> the terminal  $\text{C}_{26}$  and  $\text{C}_{27}$  methyl groups were mobile as evidenced by their elevated  $T_{1\rho}$  values in comparison with those determined from other parts of the molecule. It is noted with interest that the  $T_{1\rho}$  values of the side-chain signals up from  $\text{C}_{24}$  are particularly high for the LPC(10:0)/cholesterol mixture. However, the most significant chemical shift difference

(6) Wu, W.; Chi, L.-M. *Biochim. Biophys. Acta* **1990**, *1026*, 225-235.

(7) Oldfield, E.; Bower, J. L.; Forbes, J. *Biochemistry* **1987**, *26*, 6919-6923.

(8) Voelkel, R. *Angew. Chem., Int. Ed. Engl.* **1988**, *27*, 1468-1483.

(9) Forbes, J.; Bowers, J.; Shan, X.; Moran, L.; Oldfield, E.; Moscarello, M. A. *J. Chem. Soc., Faraday Trans. 1* **1988**, *84*, 3821-3849.

(10) Kroon, P. A.; Kainosho, M.; Chan, S. I. *Nature* **1975**, *256*, 582-584.

(11) Opella, S. J.; Yesinowski, J. P.; Waugh, J. S. *Proc. Natl. Acad. Sci. U.S.A.* **1976**, *73*, 3821-3825.

(12) Forbes, J.; Husted, C.; Oldfield, E. *J. Am. Chem. Soc.* **1988**, *110*, 1059-1065.

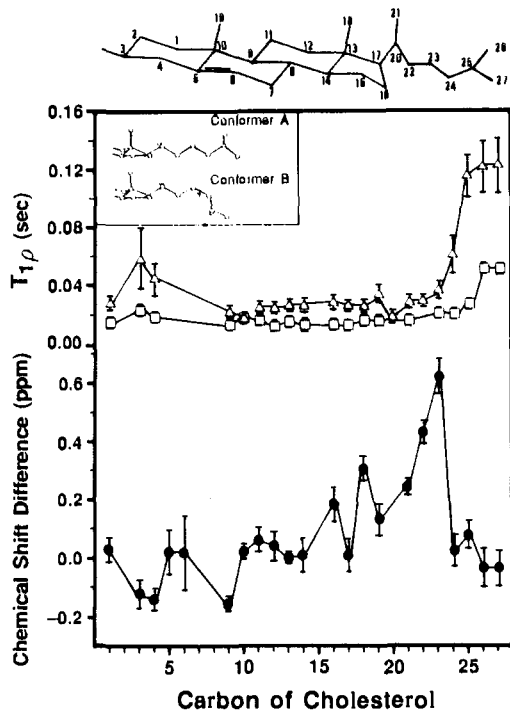


**Figure 2.**  $^{13}\text{C}$  NMR chemical shift differences and  $T_{1\rho}$  ( $^1\text{H}$ ) of LPC(10:0)/cholesterol and LPC(20:0)/cholesterol mixtures as a function of the carbon positions of the cholesterol molecule. Over 10 different contact times in the interval between 0.1 and 32 ms were used for the determination of  $T_{1\rho}$ . The error bars of the  $T_{1\rho}$  values represent the standard deviation obtained from the least-squares fitting of the intensities of spectra as a function of contact time.<sup>6</sup> The open triangle and square symbols represent  $T_{1\rho}$  obtained from LPC(10:0)/cholesterol and LPC(20:0)/cholesterol mixtures, respectively. A schematic diagram of the cholesterol molecule is shown at the top of the figure to indicate that only those signals from the terminal isooctyl side chain showed marked variation in the demonstrated NMR parameters. Two conformations of the cholesterol side chain derived from crystal structures<sup>14</sup> are also included in the figure to explain the results. The arrow shown in conformer B refers to the  $\omega_4$  ( $\text{C}_{22}$ - $\text{C}_{23}$ - $\text{C}_{24}$ - $\text{C}_{25}$ ) gauche torsion angle. A model based on the trans-to-gauche isomerization at  $\omega_4$  can explain the elevated  $T_{1\rho}$  values of the terminal  $^{13}\text{C}$  signals from  $\text{C}_{24}$  to  $\text{C}_{27}$  and the upfield displacement of the chemical shift of the  $\text{C}_{22}$  and  $\text{C}_{23}$  signals for the cholesterol side chain of the LPC(10:0)/cholesterol mixture.

was detected at  $\text{C}_{23}$ ; the  $T_{1\rho}$  values of  $\text{C}_{23}$  signals were similar to those of cholesterol condensed ring signals. Since differences in the chemical shift and  $T_{1\rho}$  of the  $^{13}\text{C}$  NMR spectrum reflect changes in the conformation and dynamics of the molecule,<sup>8</sup> some motional and conformational changes must be introduced along the  $\text{C}_{23}$ - $\text{C}_{24}$  bond of the cholesterol side chain in the LPC(10:0)-cholesterol complex.

On the basis of the  $^2\text{H}$  NMR studies on the 7/3 molar ratio of dimyristoylphosphatidylcholine/cholesterol bilayer at 25 °C, the cholesterol side chain was found to be as rigid as the condensed four-ring structure up to  $\text{C}_{22}$ .<sup>13</sup> The labeled deuterons at  $\text{C}_{24}$  were also highly ordered with probably an extended trans conformation at  $\omega_4$ . On the other hand, the 123 crystallographically independent determinations of the cholestane side chain show that the chain has four principal conformations,<sup>14</sup> of which the A and B conformers (Figure 2) are trans and gauche, respectively, for the  $\omega_4$  torsion angle. By adopting the  $\pm$ gauche form at the  $\omega_4$  torsion angle,  $\text{C}_{22}$  and  $\text{C}_{23}$  are brought to juxtaposition with the terminal carbon atoms. The observed upfield displacement of the chemical shifts of  $\text{C}_{22}$  and  $\text{C}_{23}$  signals can then be understood as the  $\gamma$ -gauche effect.<sup>15</sup> Taking all the available data together, we suggest

(13) Dufourc, E. J.; Parish, E. J.; Chitrakorn, S.; Smith, I. C. P. *Biochemistry* **1984**, *23*, 6062-6071.

(14) Duax, W. L.; Wawrzak, Z.; Griffin, J. F.; Cheer, C. In *Biology of Cholesterol*; Yeagle, Ed.; CRC Press: Boca Raton, FL, 1988; Chapter 1.

(15) Saito, H. *Magn. Reson. Chem.* **1986**, *24*, 835-852.

that the  $\omega_4$  torsion angle is trans for the cholesterol side chain of the LPC(20:0)/cholesterol mixture, whereas it undergoes trans-to-gauche isomerization for that of the LPC(10:0)/cholesterol mixture. The hydrocarbon chain length of the LPC(10:0) molecule is approximately 6 Å shorter than that of the cholesterol molecule. The cholesterol side chain may be forced to adopt a *less* extended conformation to minimize the void volume created by the LPC(10:0)-cholesterol complex in the lamellar structure.

### Synthesis of 3,4-Disubstituted Indoles via a Sequential Olefin-Insertion/Ene Route<sup>†</sup>

Jeffrey H. Tidwell, Dwayne R. Senn, and  
Stephen L. Buchwald\*

Department of Chemistry  
Massachusetts Institute of Technology  
Cambridge, Massachusetts 02139

Received December 14, 1990

Substituted indoles are structural components of a vast number of important natural products;<sup>1</sup> thus they represent attractive synthetic targets.<sup>2</sup> Historically, two approaches have been most often used for the synthesis of 3,4-disubstituted indoles. The first constructs the indole nucleus using an annelation strategy, employing a polysubstituted aromatic precursor. Included in this category are the Fischer,<sup>3</sup> Madelung,<sup>4</sup> Reissert,<sup>5</sup> and Batcho-Leimgruber<sup>6</sup> indole syntheses. In the second approach, the 3- and 4-positions of a preformed indole nucleus are selectively functionalized. Often these methods produce a mixture of regioisomers.<sup>7</sup> In this paper we report a fundamentally different route to these important molecules. Of particular significance is the complete regioselectivity of the method and its utilization of readily available starting materials.

During the past few years we have developed a general means for the generation of zirconocene complexes of substituted benzyne.<sup>8</sup> These species can serve as useful vehicles for the preparation of a variety of polysubstituted aromatic molecules via their

<sup>†</sup> This paper is dedicated to our friend and colleague Professor George Büchi, in recognition of his many notable contributions to the field of indole chemistry.

(1) (a) *The Alkaloids*; The Chemical Society: London, 1971; Specialist Periodical Reports. (b) Saxton, J. E. *Nat. Prod. Rep.* **1989**, *6*, 1. (c) Hesse, M. *Alkaloid Chemistry*; Wiley: New York, 1978. (d) Cordell, G. A. *Introduction to Alkaloids: A Biogenetic Approach*; Wiley: New York, 1981. (e) Gilchrist, T. L. *Heterocyclic Chemistry*; Pitman: London, 1981. (f) Pindur, A. R. *J. Heterocycl. Chem.* **1988**, *25*, 1.

(2) (a) Kozikowski, A. P. *Heterocycles* **1981**, *16*, 267. (b) Hegedus, L. S. *Angew. Chem., Int. Ed. Engl.* **1988**, *27*, 1113. (c) Beswick, P. J.; Greenwood, C. S.; Mowlem, T. J.; Nechvatal, G.; Widdowson, D. A. *Tetrahedron* **1988**, *44*, 7325. (d) Somei, M.; Yamada, F.; Naka, K. *Chem. Pharm. Bull.* **1987**, *35*, 1322. (e) Somei, M.; Yamada, F.; Hamada, H.; Kawasaki, T. *Heterocycles* **1989**, *29*, 643. (f) Masuda, T.; Ueda, K.; Asano, O.; Nakatsuka, S. *Heterocycles* **1987**, *26*, 1475. (g) Muratake, H.; Natsume, M. *Heterocycles* **1989**, *29*, 783. (h) Krolski, M. E.; Renaldo, A. F.; Rudisill, D. E.; Stille, J. K. *J. Org. Chem.* **1988**, *53*, 1170. (i) Moyer, M. P.; Shiurba, J. F.; Rapoport, H. J. *J. Org. Chem.* **1986**, *51*, 5106. (j) Hegedus, L. S.; Sestrick, M. R.; Michaelson, E. T.; Harrington, P. J. *J. Org. Chem.* **1989**, *54*, 4141. (k) Muratake, H.; Natsume, M. *Heterocycles* **1990**, *31*, 683.

(3) Robinson, B. *The Fischer Indole Synthesis*; Wiley-Interscience: New York, 1982.

(4) Brown, R. K. *Indoles*; Wiley-Interscience: New York, 1972. (b) Houlihan, W. J.; Parrino, V. A.; Uike, Y. *J. Org. Chem.* **1981**, *46*, 4511.

(5) Lloyd, D. H.; Nichols, D. E. *Tetrahedron Lett.* **1983**, *24*, 4561. (b) Haefliger, W.; Knecht, H. *Tetrahedron Lett.* **1984**, *25*, 285.

(6) Clark, R. D.; Repke, D. B. *Heterocycles* **1984**, *22*, 195.

(7) For instance, see: (a) Beswick, P. J.; Greenwood, C. S.; Mowlem, T. J.; Nechvatal, G.; Widdowson, D. A. *Tetrahedron* **1988**, *44*, 7325. (b) Widdowson, D. A. *Pure Appl. Chem.* **1990**, *62*, 575. (c) Somei, M.; Yamada, F.; Naka, K. *Chem. Pharm. Bull.* **1987**, *35*, 1322. (d) Somei, M.; Yamada, F.; Hamada, H.; Kawasaki, T. *Heterocycles* **1989**, *29*, 643. (e) Kogan, T. P.; Somers, T. C.; Venuti, M. C. *Tetrahedron* **1990**, *46*, 6623.

(8) Buchwald, S. L.; Nielsen, R. B. *Chem. Rev.* **1988**, *88*, 1044.